Processing Textured Surfaces via Anisotropic Geometric Diffusion

U. Clarenz, U. Diewald, M. Rumpf
Institut für Mathematik
Universität Duisburg

Abstract—**A multiscale method in surface processing is presented which carries over image processing methodology based on nonlinear diffusion equations to the fairing of noisy, textured, parametric surfaces. The aim is to smooth noisy, triangulated surfaces and accompanying noisy textures - as they are delivered by new scanning technology - while enhancing geometric and texture features. For an initial textured surface a fairing method is described which simultaneously processes the texture and the surface. Considering an appropriate coupling of the two smoothing processes one can take advantage of the frequently present strong correlations between edge features in the texture and on the surface edges. The method is based on an anisotropic curvature evolution of the surface itself and an anisotropic diffusion on the processed surface applied to the texture. Here, the involved diffusion tensors depends on a regularized shape operator of the evolving surface and on regularized texture gradients.**

A spatial finite element discretization on arbitrary unstructured triangular grids and a semi-implicit finite difference discretization in time are the building blocks of the corresponding numerical algorithm. A normal projection is applied to the discrete propagation velocity to avoid tangential drifting in the surface evolution. Different applications underline the efficiency and flexibility of the presented surface processing tool.

Keywords: Anisotropic Curvature Flow, Surface Evolution, Image Processing, Scale Space

I. Introduction

The processing of detailed triangulated surfaces is an important topic in computer aided geometric design and in computer graphics [1], [2], [3], [4]. Nowadays, various such surfaces are delivered from different measurement techniques [5] or derived from two- or three dimensional data sets [6]. Recent laser scanning technology for example enables very fine triangulation of real world surfaces and sculptures. Frequently, they are accompanied by grey or color valued texture maps. Also from medical image generation methods such as CT and MRI devices or 3D ultrasound, certain surfaces of interest can be extracted - frequently in triangulated form - at a high resolution for further post processing and analysis. Again they often come along with functional information defined on the surfaces under consideration. These surfaces and textures are usually characterized by interesting features, such as edges and corners on the geometry and in the texture intensity map. On the other hand, they are typically disturbed by noise, which is often due to local measurement errors.

The aim of this paper is to present a method which allows the *fairing of discrete surfaces coupled with the smoothing of an texture coated on the surface* and thus permits a drastic improvement of the signal to noise ratio. Additionally the approach is able to *retain and even enhance important features such as surface and texture edges and corners*. Frequently, there is a correspondence of surface and texture features. Edge features on the surface usually bound segments in the texture image, e. g. lips or hair-lines. Vice-versa jumps in the texture intensity frequently indicate geometric feature lines. Hence, we ask for a fairing method which takes advantage of this important observation and couples the fairing schemes for both quantities.

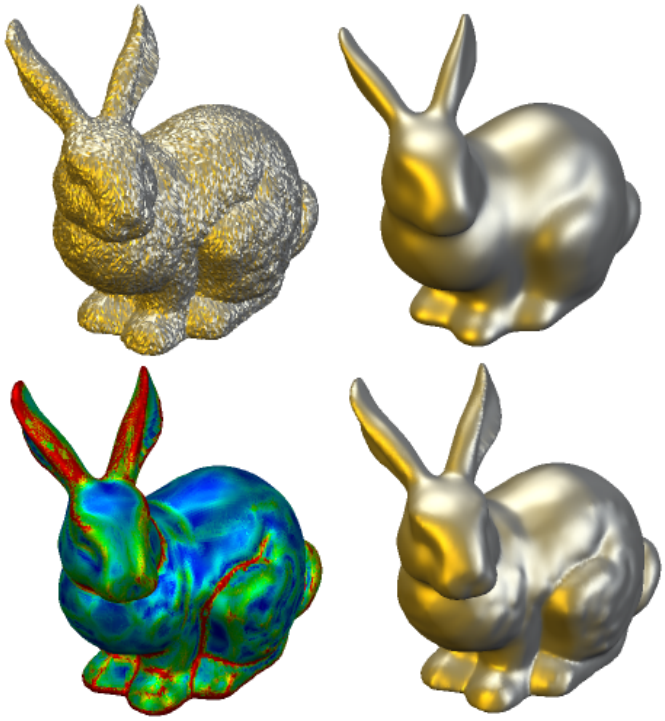

Fig. 1. *A noisy initial surface (top left) is evolved by discrete mean curvature flow (top right) and by the new anisotropic diffusion method (bottom right). Furthermore for the latter surface the dominant principal curvature - on which the diffusion tensor depends - is color coded (bottom left). The snapshots are taken at the same timesteps.*

Figure 1 shows the performance of the basic method and compares it with the a simple smoothing by mean curvature flow, the appropriate geometric "Gaussian" smoothing filter. Results on the coupled evolution of geometry and texture are given in Section V

The core of the method is a geometric formulation of scale space evolution problems for surfaces. These techniques were originally developed for image processing purposes. Thus the method not only delivers a single resulting surface, but a complete scale of surfaces in time. For increasing time, we obtain successively smoother surfaces with continuously sharpened edges and a texture depending geometry.

We derive a continuous model, which leads to a nonlinear system of parabolic partial differential equations for the coordinate mapping of the surface and for the texture. On the one hand

an anisotropic diffusion tensor depending on the shape operator and thus on the principal curvatures and principal directions of curvature, is sensitive to the identification of the important surface features. Thus, it decreases the diffusivity for the surface evolution in certain directions in close vicinity to edges or corners. The correlation of surface features with texture intensity features invokes a further pronouncing of this diffusivity control.

On the other hand, another anisotropic diffusion tensor controls the scale space evolution of the texture on the surfaces. Here, the diffusivity on the tangent space of the surface is decreased in the direction perpendicular to steep intensity gradients normal on edges in the intensity, whereas linear diffusion is allowed in tangential direction along an edge and in all directions apart from edges. Again this effect is going to be further pronounced in case of the couple evolution problem and corresponding feature direction on the geometry and in the texture. Mainly four parameters are at the disposal of the user to influence the performance of the method:

- A threshold value λ for principal curvatures which are assumed to indicate an edge and thus require local sharpening of the geometry,
- a threshold value μ for the gradient slope indicating edge intensities in the texture and thus requiring the sharpening of the intensity map, and
- filter width parameters σ and ϵ which control the noise reduction on the actual surface and texture respectively before evaluating principal curvatures and gradients.

Especially the latter is essential to make the proposed method robust and mathematically well-posed.

The method presented in this paper starts with the description of a continuous model, which has many nice qualitative properties. Then in a second step we seek a robust and efficient discretization. Hence, we derive an appropriate finite element method with respect to a formulation of the continuous problem in variational form.

The paper is organized as follows. First, in Section II we will discuss the background work on surface fairing by geometric smoothing and on image processing. In the following Section III we introduce necessary mathematical notation and discuss the basic type of geometric evolution problems. To prepare the discussion of the actual combined surface and texture diffusion model, we recall scale space methodology for images i.e. textures on surfaces in Section IV and present in Section V and VI the continuous evolution model of the separate anisotropic geometric diffusion of surfaces. The actual combination of texture and geometry diffusion is specified in Section VII. Afterwards, in Section VIII, we consider the discretized model by a suitable and effective finite element approach. The definition of a shape operator on triangulated surfaces is given in Section IX. Finally, in Section X we draw conclusions.

II. Image processing background

In physics, diffusion is known as a process that equilibrates spatial variations in concentration. If we consider some initial noisy concentration or image intensity ρ_0 on a domain $\Omega \subset \mathbb{R}^2$ and seek solutions of the linear heat equation

$$\partial_t \rho - \Delta \rho = 0 \tag{1}$$

with initial data ρ_0 and natural boundary conditions on $\partial\Omega$, we obtain a scale of successively smoothed concentrations $\{\rho(t)\}_{t\in\mathbb{R}^+}$. For $\Omega = \mathbb{R}^2$ the solution of this parabolic problem coincides with the filtering of the initial data using a Gaussian filter $\mathcal{G}_\sigma(x) = (2\pi\sigma^2)^{-1} e^{-x^2/(2\sigma^2)}$ of width or standard deviation σ, i. e. $\rho(\sigma^2/2) = \mathcal{G}_\sigma * \rho_0$. If we discretize (1) and use an explicit Euler scheme we have to compute a sequence $\{\rho^n\}_{n=0,\dots}$ with

$$\rho^{n+1} = (\mathrm{Id} + \tau\Delta_h)\rho^n$$

where τ is the timestep, Δ_h an approximation of the Laplacian and $\rho^0 = \rho_0$. Concerning the smoothing of disturbed surface geometries one may ask for analogues strategies. The geometrical counterpart of the Euclidian Laplacian Δ on smooth surfaces is the Laplace Beltrami operator $\Delta_{\mathcal{M}}$ [7], [8]. Thus, one obtains the geometric diffusion $\partial_t x = \Delta_{\mathcal{M}(t)} x$ for the coordinates x on the corresponding family of surfaces $\mathcal{M}(t)$. On triangulated surfaces as they frequently appear in geometric modeling and computer graphics applications, several authors introduced appropriate discretized operators. Taubin [4] discussed related approaches in the context of generalized frequencies on meshes and Kobbelt [2] used interpolation schemes. Explicit time discretizations are known to have strong timestep restrictions to ensure stability [9]. Thus, many iterations are required to obtain appropriate results. Kobbelt et al. [3] introduced multilevel strategies in the context of multiresolutional editing to improve the efficiency of these methods. Guskov et al. [10] discussed relaxation schemes with weights depending on the local geometry.

Recently Desbrun et al. [1] considered an implicit discretization of geometric diffusion to obtain strongly stable numerical smoothing schemes. Furthermore they improved the consistency of the discrete operator on arbitrary meshes significantly. The problem of tangential coordinate shifts on the surface, which would be a drawback of some explicit methods concerning the geometric positioning of an accompanying texture, could be avoided. The mathematical reason for such a tangential shifting of the coordinates in geometric diffusion is that the Laplace Beltrami operator depends on the metric (cf. Section III), thus the metric of the discrete surface should be kept fixed during a single explicit or implicit smoothing iteration.

¿From differential geometry [11] we know that the mean-curvature vector HN equals the Laplace Beltrami operator applied to the identity Id on a surface $\mathcal{M}$:

$$H(x)N(x) = -\Delta_{\mathcal{M}} x. \tag{2}$$

Thus geometric diffusion is equivalent to mean curvature motion (MCM)

$$\partial_t x = -H(x)N(x)\ , \tag{3}$$

where $H(x)$ is the corresponding mean curvature (here defined as the sum of the two principal curvatures), and $N(x)$ is the normal on the surface at point x. Already in '91 Dziuk [12] presented a semi implicit finite element scheme for MCM on triangulated surface. The approach by Desbrun et al. [1] is essentially identical to this earlier method.

Fig. 2. *Isotropic Perona-Malik diffusion (right) is applied to a noisy initial image (left).*

Unfortunately MCM doesn't only decrease the geometric noise due to unprecise measurement but also smoothes out geometric features such as edges and corners of the surface. Hence, we seek models which improve a simple high pass filtering.

In image processing, Perona and Malik [13] proposed a nonlinear diffusion method, which modifies the diffusion coefficient at edges. Edges are indicated by steep intensity gradients. For a given initial image ρ_0 they considered the evolution problem

$$\partial_t \rho - \operatorname{div}\left(G\left(\frac{\|\nabla\rho\|}{\lambda}\right)\nabla\rho\right) = 0 \tag{4}$$

for some parameter $\lambda \in \mathbb{R}^+$. For increasing time t - the scale parameter - the original image at the initial time is now successfully smoothed and image patterns are coarsened. But simultaneously edges are enhanced if one chooses a diffusion coefficient $G(.)$ which suppresses diffusion in areas of high gradients (cf. Fig. 2). A suitable choice for G is

$$G(s) = \left(1 + s^2\right)^{-1} . \tag{5}$$

Thus edges are classified by the involved parameter λ.

Kawohl and Kutev [14] gave a detailed analysis of the diffusion types in this method. In the axiomatic work by Alvarez et al. [15], general nonlinear diffusion problems have been introduced. More precisely they derive parabolic equations with elliptic terms which are based on the curvature of isolines or isosurfaces in images.

Unfortunately the above original Perona and Malik model is still ill-posed because there is a true backward diffusion in areas of large gradients. Catté et al. [16] proposed a regularization method where the diffusion coefficient is no longer evaluated on the exact intensity gradient. Instead they suggested to consider the gradient evaluation on a prefiltered image, i.e., they consider the equation

$$\partial_t \rho - \operatorname{div}\left(G\left(\frac{\|\nabla\rho_\sigma\|}{\lambda}\right)\nabla\rho\right) = 0 \tag{6}$$

where $\rho_\sigma = \mathcal{G}_\sigma * \rho$ with a suitable local convolution kernel $\mathcal{G}_\sigma$, e.g. an Gaussian filter kernel. This model turns out to be well-posed, edges are still enhanced. The evolution and the prefiltering avoid the detection and pronouncing of initial noise as artificial edges.

Weickert [17] improved this method taking into account anisotropic diffusion, where the Perona Malik type diffusion is concentrated in one direction, for instance the gradient direction of a prefiltered image. This leads to an additional tangential smoothing along edges and amplifies intensity correlations along lines. Preußer and Rumpf [18] took up this idea for the construction of streamline type patterns in flow fields. Kimmel [19] generalized the scale space approach for planar images to the case of images mapped on surfaces (cf. Section IV). For a nice exposition and further references on geometric concepts in image processing we refer to the book of Sapiro [20].

Concerning the numerical implementation beyond many other authors Weickert proposed finite difference schemes [21] and Kačur and Mikula [22] suggested a semi-implicit finite element implementation for the isotropic model by Catté et al., Bänsch and Mikula [23] as well as Preußer and Rumpf [24] discussed adaptive finite element methods in 2D and 3D image processing by anisotropic nonlinear diffusion. In [25] a finite element implementation of a level set method for anisotropic geometric diffusion is discussed which is closely related to the parametric surface evolution problem presented here.

III. Geometric evolution problems revisited

Before we develop our model of nonlinear geometric surface processing, let us first briefly review the basic notation of manifolds, differential calculus and geometric diffusion. For a detailed introduction into geometry and differential calculus we refer to [7] and [8, Chapter 1]. For the sake of simplicity we assume our surfaces to be compact embedded manifolds without boundaries. Thus we consider a smooth manifold $\mathcal{M}$, which we suppose to be embedded in $\mathbb{R}^3$. By (x, Ω) we denote a chart of $\mathcal{M}$, where $\Omega \subset \mathbb{R}^2$ is an open reference domain and

$$x : \Omega \to \mathcal{M} \,;\, \xi \mapsto x(\xi)$$

is the corresponding coordinate map. For each point x on $\mathcal{M}$ a tangent space $\mathcal{T}_x\mathcal{M}$ is spanned by the basis $\{\frac{\partial}{\partial\xi_1}, \frac{\partial}{\partial\xi_2}\}$. We regard tangent vectors as linear functionals on $C^\infty(\mathcal{M})$, i. e. for $f \in C^\infty(\mathcal{M})$ we define

$$\frac{\partial}{\partial\xi_i}(x) f := \frac{\partial f(x)}{\partial\xi_i}(\xi)$$

where $x = x(\xi)$. Due to the embedding in $\mathbb{R}^3$ we identify $\frac{\partial}{\partial\xi_i}$ with the tangent vector $\frac{\partial x}{\partial\xi_i}$. By $\mathcal{TM}$ we denote the tangent bundle. Integration on $\mathcal{M}$ requires the definition of a metric $g(\cdot,\cdot) : \mathcal{T}_x\mathcal{M} \times \mathcal{T}_x\mathcal{M} \to \mathbb{R}$, where g is supposed to be a quadratic positive definite form. In our embedded - i.e. especially immersed - case we obtain a representation $(g_{ij})_{ij}$ with respect to the basis $\{\frac{\partial}{\partial\xi_1}, \frac{\partial}{\partial\xi_2}\}$ of g

$$g_{ij} = g(\frac{\partial}{\partial\xi_i}, \frac{\partial}{\partial\xi_j}) = \frac{\partial x}{\partial\xi_i} \cdot \frac{\partial x}{\partial\xi_j} , \tag{7}$$

where $\cdot$ indicates the scalar product in $\mathbb{R}^3$. The inverse of $(g_{ij})_{ij}$ is denoted by $(g^{ij})_{ij}$.

Integrating either a product of two functions f, g on $\mathcal{M}$ or the product of two vector fields v, w on $\mathcal{TM}$ we obtain the follow-

ing scalar products on $C^0(\mathcal{M})$ and $C^0(\mathcal{TM})$, respectively:

$$(f,g)_{\mathcal{M}} := \int_{\mathcal{M}} fg \; \mathrm{d}x \,, \quad (v,w)_{\mathcal{TM}} := \int_{\mathcal{M}} g(v,w) \; \mathrm{d}x \,.$$

As the closure of $C^\infty(\mathcal{M})$ with respect to the induced norm $||\cdot||_{L^2(\mathcal{M})} = \sqrt{(\cdot,\cdot)_{\mathcal{M}}}$ we obtain $L^2(\mathcal{M})$.

Next we proceed considering the fundamental differential operators on $\mathcal{M}$. Suppose $f \in C^1(\mathcal{M})$ then the total differential *df* is a linear functional on $\mathcal{TM}$ ($df \in \mathcal{TM}'$), i. e. $\langle \frac{\partial}{\partial \xi_i}, df \rangle_{x(\xi)} := \frac{\partial (f \circ x)}{\partial \xi_i}(\xi)$. The gradient $\nabla_{\mathcal{M}} f$ of f is defined as the representation of *df* with respect to the metric g: $g\left(\nabla_{\mathcal{M}} f, \frac{\partial}{\partial \xi_i}\right) = \left\langle \frac{\partial}{\partial \xi_i}, df \right\rangle$. In coordinates we obtain

$$\nabla_{\mathcal{M}} f = \sum_{i,j} g^{ij} \frac{\partial (f \circ x)}{\partial \xi_j} \frac{\partial}{\partial \xi_i} \,. \tag{8}$$

Furthermore, the divergence $\mathrm{div}_{\mathcal{M}} v$ for a vector field $v \in \mathcal{TM}$ is defined as the dual operator of the gradient by

$$\int_{\mathcal{M}} \phi \, \mathrm{div}_{\mathcal{M}} v \; \mathrm{d}x := - \int_{\mathcal{M}} g(\nabla_{\mathcal{M}} \phi, v) \; \mathrm{d}x \tag{9}$$

for all $\phi \in C_0^\infty(\mathcal{M})$. In local coordinates we have the following representation of the divergence. Let $v = v^i \frac{\partial}{\partial \xi_i}$; then $\mathrm{div}_{\mathcal{M}} v$ can be represented as:

$$\mathrm{div}_{\mathcal{M}} v = \frac{1}{\sqrt{\det(g_{ij})}} \frac{\partial}{\partial \xi_i} (\sqrt{\det(g_{ij})}\, v^i) \,. \tag{10}$$

Once we have introduced the gradient of a function on $\mathcal{M}$, we directly obtain the Dirichlet form $(\nabla_{\mathcal{M}} u, \nabla_{\mathcal{M}} v)_{\mathcal{TM}}$.

The closure of the $C^\infty(\mathcal{M})$ with respect to the induced norm

$$(u,u)_{H^1(\mathcal{M})} = \sqrt{||u||^2_{L^2(\mathcal{M})} + (\nabla_{\mathcal{M}} u, \nabla_{\mathcal{M}} u)_{\mathcal{TM}}}$$

is denoted $H^1(\mathcal{M})$. Furthermore, the weak Laplace Beltrami operator $\Delta_{\mathcal{M}}$ applied to any function $u \in H^1(\mathcal{M})$ is defined as a functional on $H^1(\mathcal{M})$ making use of the duality

$$(-\Delta_{\mathcal{M}} u, \phi)_{\mathcal{M}} := (\nabla_{\mathcal{M}} u, \nabla_{\mathcal{M}} \phi)_{\mathcal{TM}} \tag{11}$$

for all $\phi \in H^1(\mathcal{M})$. Using (8) and (10) we obtain the following representation of $\Delta_{\mathcal{M}} u$ in local coordinates for a smooth function u:

$$\Delta_{\mathcal{M}} u = \sum_{i,j} \frac{1}{\sqrt{\det(g_{ij})}} \frac{\partial}{\partial \xi_i} \left(g^{ij} \sqrt{\det(g_{ij})} \frac{\partial u}{\partial \xi_j} \right) \,.$$

In the anisotropic diffusion method to be presented in this paper we will make intensive use of some fundamental curvature quantities. Let us assume that $\mathcal{M}$ is orientable; then we have a well defined normal $N : \mathcal{M} \to S^2 \subset \mathbb{R}^3$ on $\mathcal{M}$. Using the notation $\frac{\partial x}{\partial \xi_j} = x_{,j}$ the second fundamental form $II : \mathcal{T}_x\mathcal{M} \times \mathcal{T}_x\mathcal{M} \to \mathbb{R}$ is locally given by

$$II(v,w) := - \sum_{i,j} v^i w^j \, h_{ij} := \sum_{i,j} v^i w^j \, N_{,i} \cdot x_{,j} \,,$$

where the Gauss map $N : \Omega \to S^2$ is a representation of the normal with respect to a coordinate map $x : \Omega \to \mathcal{M}$ and $v = v^1 \frac{\partial}{\partial \xi_1} + v^2 \frac{\partial}{\partial \xi_2}$, $w = w^1 \frac{\partial}{\partial \xi_1} + w^2 \frac{\partial}{\partial \xi_2}$, are two tangent vectors in $\mathcal{T}_x\mathcal{M}$. We point out that II is well defined, i. e. it is invariant under reparametrization. Furthermore, II is a symmetric bilinear form and therefore there is a symmetric endomorphism $S_{\mathcal{T}_x\mathcal{M}} : \mathcal{T}_x\mathcal{M} \to \mathcal{T}_x\mathcal{M}$ such that

$$g(S_{\mathcal{T}_x\mathcal{M}} v, w) = II(v,w) \,; \; v,w \in \mathcal{T}_x\mathcal{M} \,.$$

The endomorphism $S_{\mathcal{T}_x\mathcal{M}}$ is called shape operator. Its eigenvalues are the principal curvatures of $\mathcal{M}$ at the point x and the eigenvectors are the principal directions of curvature. Now, one can define notions of curvature such as the *mean-curvature* H and the *Gaussian curvature* K by

$$H := \mathrm{tr}\, S_{\mathcal{T}_x\mathcal{M}} \,, \quad K := \det S_{\mathcal{T}_x\mathcal{M}} \,. \tag{12}$$

(Note that in our notation the mean-curvature H is the sum instead of the arithmetic mean of the principal curvatures.) With the Laplace Beltrami operator at hand we can finally introduce a geometric diffusion problem in analogy to the linear diffusion problem in Euclidian space. We seek a solution $u : \mathbb{R}_0^+ \times \mathcal{M} \to \mathbb{R}$ of the parabolic equation $\partial_t u(t,x) - \Delta_{\mathcal{M}} u(t,x) = 0$ on $\mathbb{R}_0^+ \times \mathcal{M}$ for given initial data $u(0,\cdot) = u_0$. Here, u_0 is some function on $\mathcal{M}$. Furthermore, we can consider a diffusion of the manifold geometry itself (cf. Section II). I. e., we seek a one parameter family of embedded manifolds $\{\mathcal{M}(t)\}_{t \geq 0}$ and corresponding parametrizations $x(t)$, such that

$$\begin{aligned} \partial_t x(t) - \Delta_{\mathcal{M}(t)} x(t) &= 0 \,, \\ \mathcal{M}(0) &= \mathcal{M}_0 \,. \end{aligned} \tag{13}$$

For the sake of simplicity we define $MCM(\mathcal{M}_0, t) := \mathcal{M}(t)$, where $\mathcal{M}(t)$ is the solution surface at time t. Thus $MCM(\mathcal{M}, \sigma^2/2)$ can be regarded as the application of a "geometric " Gaussian filter of width σ to $\mathcal{M}$. Applying integration by parts, we obtain

$$(\partial_t x, \theta)_{\mathcal{M}(t)} + (\nabla_{\mathcal{M}(t)} x, \nabla_{\mathcal{M}(t)} \theta)_{\mathcal{TM}(t)} = 0 \,. \tag{14}$$

This is the corresponding weak variational formulation which holds for all test functions $\theta \in [C^\infty(\mathcal{M}(t))]^3$. The fundamental observation is that this geometric diffusion of the coordinate mapping itself coincides with the motion by mean curvature (MCM); in fact for any manifold $\mathcal{M}$ we have $\Delta_{\mathcal{M}} x = -H(x)\, N(x)$ as already stated above in Section II.

IV. Anisotropic diffusion for textures on fixed surfaces

The aim of this section is to recall scale space methods for images now given as maps on manifolds. The concepts from the Euclidian case of planar images can be inherited to the Riemannian case of textures on fixed surfaces (cf. Kimmel [19]). We simply have to replace the involved differential operators form the Euclidian setting by the corresponding differential operators on manifolds. Here we already transcribe the basic anisotropic diffusion method introduced by Weickert [26] to define an anisotropic texture diffusion on a given manifold that retains edge features in the texture and simultaneously allows for

tangential smoothing along the edge line on the fixed surface. Thus, let

$$u_0 : \mathcal{M} \to \mathbb{R} \tag{15}$$

be a given texture on a fixed surface $\mathcal{M}$. We consider the following diffusion process:

$$\begin{aligned} \partial_t u(t) - \mathrm{div}_{\mathcal{M}}(b^\epsilon \nabla_{\mathcal{M}} u(t)) &= 0, \\ u(0) &= u_0, \end{aligned}$$

where the diffusion tensor b^ϵ is supposed to be a positive definite endomorphism on the tangent bundle $\mathcal{T}_x\mathcal{M}$ for every $x \in \mathcal{M}$. The superscript ϵ indicates a regularization involved in the evaluation of the diffusivity. Thus we apply a Gaussian filter of width ϵ to the current texture map $u(t)$ before we compute gradients. I.e. we define u^ϵ as the solution of the parabolic initial value problem $\partial_t u(t) - \Delta_{\mathcal{M}} u(t) = 0$ on $\mathcal{M}$ with initial data $u(0) = u_0$ at time $t = \epsilon^2/2$. In matrix representation with respect to the basis $\{v_1 = \frac{\nabla_{\mathcal{M}} u^\epsilon}{\|\nabla_{\mathcal{M}} u^\epsilon\|}, v_2 = v_1^\perp\}$ we obtain

$$b^\epsilon = \begin{pmatrix} G\left(\frac{\|\nabla_{\mathcal{M}} u^\epsilon\|}{\mu}\right) & 0 \\ 0 & 1 \end{pmatrix} \tag{16}$$

for some edge indicating parameter $\mu \in \mathbb{R}^+$. As nonlinearity $G(\cdot)$ we consider the function already given in (5). Let us emphasize that for vanishing gradients $\nabla_{\mathcal{M}} u^\epsilon$ the diffusion tensor b^ϵ tends to the identity on $T_x\mathcal{M}$ and we locally more or less end up with linear diffusion in regions apart from texture edges.

V. Anisotropic geometric diffusion

We are now prepared to discuss the concept of anisotropic geometric diffusion as a powerful multiscale method for the processing of the surface geometry itself. The aim is to appropriately carry over approved methodology from scale space theory in image processing, now not only applied to image intensities *on* surfaces but to the surface itself. Here we restrict ourselves to the smoothing of a noisy surface without texture. Preliminary results on this restricted case have been presented in [27]. In the following paragraph especially an considerable implementational improvement based on the splitting in tangential and normal velocity components is presented. For the general case coupling surface and texture evolution we refer to Section VII. Let us first summarize the building blocks of the method:

- We consider a noisy initial surface $\mathcal{M}_0$ to be smoothed. Thus we replace the linear diffusion from the Euclidian case of flat images by an appropriate anisotropic diffusion of the surface geometry itself. Thereby a family of surfaces $\{\mathcal{M}(t)\}_{t\in\mathbb{R}_0^+}$ is generated, where the time t serves as the scale parameter.
- In addition to the smoothing of the surface, our aim is to maintain or even enhance sharp edges of the surface. The canonical quantity for the detection of edges is the curvature tensor, in the case of codimension 1 represented by the symmetric shape operator $S_{\mathcal{T}_x\mathcal{M}}$. An edge is supposed to be indicated by one sufficiently large eigenvalue of $S_{\mathcal{T}_x\mathcal{M}}$. Hence we consider a diffusion tensor depending on $S_{\mathcal{T}_x\mathcal{M}}$, which enables us to decrease diffusion significantly at edges indicated by $S_{\mathcal{T}_x\mathcal{M}}$. Furthermore we will introduce a threshold parameter λ as in (4) for the identification of edges.
- The evaluation of the shape operator on a noisy surface might be misleading with respect to the original but unknown surface and its edges. Thus we prefilter the current surface $\mathcal{M}(t)$ before we evaluate the shape operator. The straightforward "geometric Gaussian" filter is a short timestep of mean curvature flow. Hence, we compute a shape operator $S^\sigma_{\mathcal{T}_x\mathcal{M}}$ on the resulting prefiltered surface $\mathcal{M}_\sigma(t)$, where the parameter σ is the "geometric Gaussian" filterwidth, i.e. $\mathcal{M}_\sigma(t) = MCM(\mathcal{M}(t), \sigma^2/2)$. Let us emphasize that this choice also leads to a mathematically well-posed parabolic problem. Hence we avoid ill-posed backward diffusion in our model.
- With an appropriately chosen scalar diffusion coefficient depending on the eigenvalues $\kappa^{1,\sigma}, \kappa^{2,\sigma}$ of $S^\sigma_{\mathcal{T}_x\mathcal{M}}$, which are the principal curvatures of $\mathcal{M}_\sigma(t)$, it is already possible to smooth in approximately flat surface areas and to enhance edges somewhere else. Along these edges the surfaces $\mathcal{M}(t)$ still retains its noisy structure from $\mathcal{M}_0$ (cf. Fig. 3). We incorporate anisotropic diffusion now based on a proper diffusion tensor $a^\sigma_{\mathcal{T}_x\mathcal{M}}$ which enables tangential smoothing along edges. Thereby, the tangential edge direction on the tangent space $\mathcal{T}_x\mathcal{M}(t)$ is indicated by the principal direction of curvature corresponding to the subdominant principal curvature. The second, perpendicular direction is considered to be the actual sharpening direction. Figure 3 clearly outlines the advantage of an anisotropic diffusion tensor.
- The resulting method leads to spatial displacement and the volume enclosed by $\mathcal{M}(t)$ is changed in the evolution. Introducing an additional force f in the evolution which depends on certain integrated curvature expressions leads to volume preservation and we can further improve our multiscale method (see Section VI).

We end up with the following type of parabolic surface evolution problem. Given an initial compact embedded manifold $\mathcal{M}_0$ in $\mathbb{R}^3$, we compute a one parameter family of manifolds $\{\mathcal{M}(t)\}_{t\in\mathbb{R}_0^+}$ with corresponding coordinate mappings $x(t)$ which solves the system of anisotropic geometric evolution equations (which generalizes the system (13)):

$$\partial_t x - \mathrm{div}_{\mathcal{M}(t)}(a^\sigma_{\mathcal{T}_x\mathcal{M}} \nabla_{\mathcal{M}(t)} x) = f \ \text{ on } \ \mathbb{R}^+ \times \mathcal{M}(t), \tag{17}$$

and satisfies the initial condition

$$\mathcal{M}(0) = \mathcal{M}_0.$$

Here, for every point x on $\mathcal{M}(t)$ the diffusion tensor $a^\sigma_{\mathcal{T}_x\mathcal{M}}$ is supposed to be a symmetric, positive definite, linear mapping on the tangent space $\mathcal{T}_x\mathcal{M}$:

$$a^\sigma_{\mathcal{T}_x\mathcal{M}}(x) : \mathcal{T}_x\mathcal{M} \to \mathcal{T}_x\mathcal{M} \ .$$

Furthermore, f represents the forcing on the right-hand side that maintains certain geometric properties of $\mathcal{M}(t)$.

In the simplest model we consider an isotropic scalar diffusion coefficient and set

$$a^\sigma_{\mathcal{T}_x\mathcal{M}} = G\left(\frac{\sqrt{(\kappa^{1,\sigma})^2 + (\kappa^{2,\sigma})^2}}{\lambda}\right) \mathrm{Id}, \tag{18}$$

for the function G which was introduced for the nonlinear diffusion on planar images (cf. (5)) and a control parameter $\lambda \in \mathbb{R}^+$.

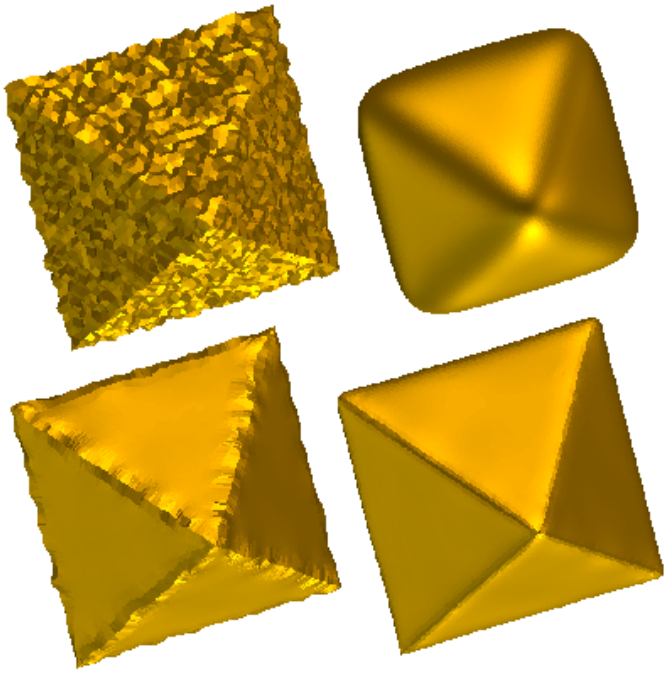

Fig. 3. *Comparison of different surface evolution models applied to the initially noisy surface depicted on top left. On the top right the result of the mean curvature motion* (13) *is shown. On the bottom left the result employing the new isotropic diffusion coefficient* (18) *and on the bottom right the resulting surface under the new edge preserving anisotropic evolution using the diffusion coefficient* (19) *are shown. The different results are evaluated for the same time* $t = 0.0032$ *and the parameters where chosen as* $\sigma = 0.02$ *and* $\lambda = 5$. *The diameter of initial surface is chosen to be* 1.

As already announced, an improved model integrates tangential smoothing along edges into the multiscale approach. Therefore we consider an anisotropic diffusion tensor $a^\sigma_{\mathcal{T}_x\mathcal{M}}$ which is no longer restricted to multiples of the identity and which doesn't lead to a scalar diffusion coefficient. There is an orthonormal basis $\{w^1, w^2\}$ of $\mathcal{T}_x\mathcal{M}_\sigma$ such that $S^\sigma_{\mathcal{T}_x\mathcal{M}_\sigma}$ is represented by

$$S^\sigma_{\mathcal{T}_x\mathcal{M}_\sigma} = \begin{pmatrix} \kappa^{1,\sigma} & 0 \\ 0 & \kappa^{2,\sigma} \end{pmatrix}$$

because of the symmetry of the shape operator. Now we consider a diffusion tensor in equation (17) which is defined as follows with respect to the above orthonormal basis. First we introduce a diffusion on $\mathcal{T}_x\mathcal{M}_\sigma$ in the basis $\{w^1, w^2\}$ as

$$a^\sigma_{\mathcal{T}_x\mathcal{M}_\sigma} = a(S^\sigma_{\mathcal{T}_x\mathcal{M}_\sigma}) = \begin{pmatrix} G\left(\frac{\kappa^{1,\sigma}}{\lambda}\right) & 0 \\ 0 & G\left(\frac{\kappa^{2,\sigma}}{\lambda}\right) \end{pmatrix} \tag{19}$$

with the function G from above. Finally, to define the actual diffusion on $\mathcal{T}_x\mathcal{M}$ we decompose a vector $z \in \mathbb{R}^3$ in the orthogonal basis $\{w^1, w^2, N^\sigma\}$, i. e.

$$z = (z \cdot w^1)w^1 + (z \cdot w^2)w^2 + (z \cdot N^\sigma)N^\sigma$$

where $\{w^1, w^2\} \subset \mathbb{R}^3$ denotes the embedded tangent vectors corresponding to the above basis w^1, w^2 and N^σ is the surface normal of $\mathcal{M}_\sigma$. Then we define the diffusion coefficient $a^\sigma_{\mathcal{T}_x\mathcal{M}}$ by

$$a^\sigma_{\mathcal{T}_x\mathcal{M}}\, z := \Pi_{T_x M}\Big(G(\kappa^{1,\sigma})(z \cdot w^1)w^1 + G(\kappa^{2,\sigma})(z \cdot w^2)w^2 + (z \cdot N^\sigma)N^\sigma\Big). \tag{20}$$

Here $\Pi_{\mathcal{T}_x\mathcal{M}}$ denotes the orthogonal projection onto the tangent space $\mathcal{T}_x\mathcal{M}$.

Hence, due to the anisotropy defined in (19), we enforce a signal enhancement in a principal direction of curvature with curvature larger than λ. If the second principal curvature is smaller than λ we regard the first direction as orthogonal to an important edge on the surface which is going to be sharpened. Simultaneously, in the other direction - the tangent direction along the edge - we allow smoothing. At corners both principal curvatures are large, thus sharpening takes place in both directions.

In variational formulation the evolution problem (17) is given by

$$(\partial_t x, \theta)_{\mathcal{M}(t)} + (a^\sigma_{\mathcal{T}_x\mathcal{M}}\, \nabla_{\mathcal{M}(t)} x, \nabla_{\mathcal{M}(t)}\theta)_{\mathcal{T}\mathcal{M}(t)} = (f, \theta)_{\mathcal{M}(t)}\,, \tag{21}$$

for all $\theta \in [C^\infty(\mathcal{M}(t))]^3$. We can express the above equation not only in variational form but also in coordinates (cf. equations (8) and (10)):

$$\partial_t x - \sum_{i,j,k,l} \frac{1}{\sqrt{\det(g_{ij})}}\, \frac{\partial}{\partial \xi_i}\left(\sqrt{\det(g_{ij})}\; g^{ij} a^\sigma_{jk} g^{kl} \frac{\partial x}{\partial \xi_l}\right) = f$$

on $\mathbb{R}^+ \times \mathcal{M}(t)$, where $a^\sigma_{jk} = g\left(a^\sigma_{\mathcal{T}_x\mathcal{M}} \frac{\partial}{\partial \xi_j}, \frac{\partial}{\partial \xi_k}\right)$. We will nevertheless focus on the variational formulation - especially when we implement a suitable finite element algorithm.

For $f = 0$ and vanishing regularization parameter σ, we can rewrite the evolution problem (see [28])

$$\partial_t x = -H_{a^\sigma_{\mathcal{T}_x\mathcal{M}}}\, N + (\mathrm{div}_{\mathcal{M}}\, a^\sigma_{\mathcal{T}_x\mathcal{M}})(x)\,,$$

Here we denote by

$$H_{a^\sigma_{\mathcal{T}_x\mathcal{M}}} := \mathrm{tr}\,(a^\sigma_{\mathcal{T}_x\mathcal{M}} \circ S^\sigma_{\mathcal{T}_x\mathcal{M}_\sigma})$$

a generalization of the classical mean curvature. In general we proceed as follows

Let $a : \mathcal{T}_x\mathcal{M} \to \mathcal{T}_x\mathcal{M}$ be an endomorphism of the tangent space. The corresponding a-mean curvature H_a is given as

$$H_a := \mathrm{tr}\,(a \circ S)\,,$$

where S is the shape operator on $\mathcal{M}$.

Hence $\partial_t x$ splits into a tangential component and a component orthogonal to the surface,

$$\begin{aligned} \Pi_{(\mathcal{T}_x\mathcal{M})^\perp}\, \partial_t x &= -H_{a^\sigma_{\mathcal{T}_x\mathcal{M}}} N \\ \Pi_{\mathcal{T}_x\mathcal{M}}\, \partial_t x &= (\mathrm{div}_{\mathcal{M}}\, a^\sigma_{\mathcal{T}_x\mathcal{M}})(x)\,. \end{aligned}$$

Here $\Pi_{(\mathcal{T}_x\mathcal{M})^\perp} V = \langle V\,, N\rangle\, N$ (with N being the surface normal), is the orthogonal projection onto the normal-space of the surface, and $\Pi_{\mathcal{T}_x\mathcal{M}} V = V - \Pi_{(\mathcal{T}_x\mathcal{M})^\perp} V$ is the corresponding projection onto the tangent-space.

The tangential part $\Pi_{T_x\mathcal{M}}\,\partial_t x$ causes a tangential drift of the surface coordinates on the surface but it does not influence the shape of the surface itself. Nevertheless this property may result in degeneration of triangles in the case of discrete surfaces, c.f. Figure 9. To avoid this problem we reformulate (17) by

$$\partial_t x - \Pi_{(T_x\mathcal{M})^\perp}\,\mathrm{div}_{\mathcal{M}}\left(a^\sigma_{T_x\mathcal{M}}\,\nabla_{\mathcal{M}} x\right) = \Pi_{(T_x\mathcal{M})^\perp} f\ . \qquad (22)$$

Cf. Figure 10 for numerical results using this evolution formulation.

VI. Volume conservation

The volume enclosed by a surface without boundary is an important characteristic, which we should try to preserve during processing. Using the following Theorem it is possible to define an algorithm for image processing that keeps the volume enclosed by the considered surface fixed.

Theorem 1: Let $a : \mathcal{T}_x\mathcal{M} \to \mathcal{T}_x\mathcal{M}$ be an endomorphism of the tangent-space in every point on $\mathcal{M}$. Then the enclosed volume of the surface does not change under the evolution

$$\partial_t x - \mathrm{div}_{\mathcal{M}}\left(a\,\nabla_{\mathcal{M}} x\right) = h(t)N$$

if we choose $h(t) := \frac{1}{\int_{\mathcal{M}(t)} dx}\int_{\mathcal{M}(t)} H_a\ \mathrm{d}x$.

The proof of the above Theorem is analogues to the one given in case of mean curvature motion in [29]. Using the notion of the $a^\sigma_{T_x\mathcal{M}}$-mean curvature $H_{a^\sigma_{T_x\mathcal{M}}}$, we can express the changing-rate of the area $\mathrm{Ar}(\mathcal{M}(t))$ and the volume $\mathrm{Vol}(\mathcal{M}(t))$ enclosed by the compact surface $\mathcal{M}(t)$. Here $\mathcal{M}(t)$ is assumed to be the solution of the homogeneous evolution problem $\partial_t x - \mathrm{div}_{\mathcal{M}(t)}(a^\sigma_{T_x\mathcal{M}}\,\nabla_{\mathcal{M}(t)} x) = 0$:

$$\begin{aligned}\frac{d}{dt}[\mathrm{Ar}(\mathcal{M}(t))]_{t=t_0} &= -\int_{\mathcal{M}(t_0)} H\,H_{a^\sigma_{T_x\mathcal{M}}}\ \mathrm{d}x\,,\\ \frac{d}{dt}[\mathrm{Vol}(\mathcal{M}(t))]_{t=t_0} &= -\int_{\mathcal{M}(t_0)} H_{a^\sigma_{T_x\mathcal{M}}}\ \mathrm{d}x\,.\end{aligned}$$

The first equation underlines the smoothing effect in our model. There is a significant regularization, indicated by the area minimization in areas which are expected to be rather flat based on the classification after the prefiltering. The second equation is the key in the definition of a volume preserving force term f on the right hand side. To achieve this we have to select a function f which compensates the overall change in volume by a constant forcing in normal direction, i. e., we consider the force f given in the above theorem. Alternatively and much simpler, we can select a retrieving force

$$f(t,x) = C\,(x_0 - x(t)) \qquad (23)$$

where x_0 is the original point location on the initial surface $\mathcal{M}_0$. This will keep the surface close to the initial surface but in general does not guarantee any conservation principle.

VII. Coupling anisotropic texture and surface diffusion

Up to now, we have considered anisotropic diffusion for noisy textures on fixed surfaces (cf. Section IV) and for noisy surfaces without texture (cf. Section V). Recalling our original intention we now focus on the coupling of these two diffusion processes, making use of characteristic correlations between surface and texture features. Usually textures are colour valued maps. For the ease of presentation we confine here to an exposition of grey valued intensities. In the vector valued case of colour textures one proceeds along the line described in [30]. Let us emphasize that the choice of a suitable colour model is of particular importance for the appropriateness of the results. For a discretion of the *RGB*- or *HSV*-colour model we refer to [31]. The figures depicted here already show colour textures.

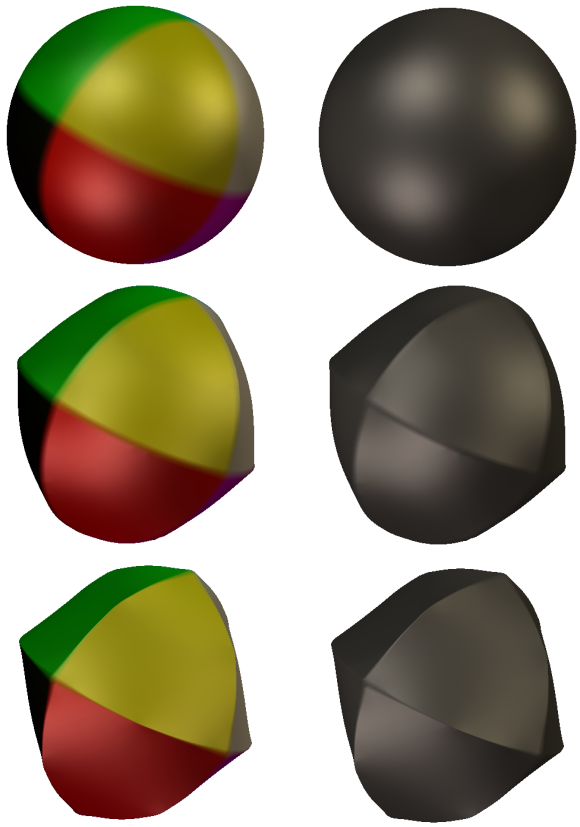

Fig. 4. *Example for the evolution of a surface with texture information under the combined diffusion* (24) *and* (26)*. Because of the dependency of the diffusion coefficient a_G on the texture during the evolution geometry edges develop in areas of high texture gradients. The parameters are chosen as $\tau = 0.00001$, $\sigma = 0.0045$, $\lambda = 20$, $\mu = 2$, and the diameter of the surface is scaled to 1. On top the initial surface is shown with and without texture information, below two timesteps for $t = 0.000015$ and $t = 0.00003$ are depicted.*

As explained in the introduction we aim to intensify the modulation of the diffusivity as well in the surface as in the texture diffusion model whenever edge type features are detected not only in the one but also simultaneously in the other quantity.

Hence, for the surface evolution we decompose the texture intensity gradient with respect to the coordinate system aligned to the principal directions of curvature on the surface and vice versa for texture diffusion the curvature directions are decomposed into the directions of the texture gradient and perpendicular to it:

If the texture gradient points in the direction of the dominant curvature we further reduce the diffusivity in this direction. Analogously we reduce the diffusion coefficient corresponding

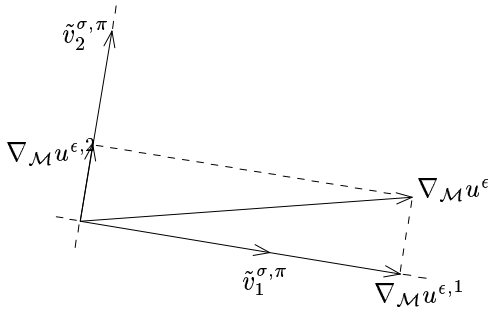

Fig. 5. *Decomposition of the texture gradient $\nabla_{\mathcal{M}} u^{\epsilon}$ into the components parallel to the two principal directions of curvature $\tilde{v}^{1,\sigma,\pi}, \tilde{v}^{2,\sigma,\pi}$.*

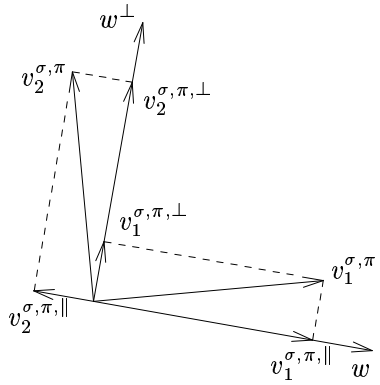

Fig. 6. *Decomposition of the two principal directions of curvature $v^{1,\sigma,\pi}, v^{2,\sigma,\pi}$ into the components parallel and orthogonal to w.*

to the texture gradient direction if the geometry is significantly curved in this direction.

In what follows we will give the details separately for the surface and texture diffusion problem.

Respecting texture features in the surface evolution

Let us start considering the local situation near a geometry edge with principal curvatures $\kappa^{1,\sigma}$, $\kappa^{2,\sigma}$ and $\left|\kappa^{1,\sigma}\right| \gg \left|\kappa^{2,\sigma}\right|$. The principal direction of curvature $v^{2,\sigma}$ corresponding to the curvature $\kappa^{2,\sigma}$ points along the geometry edge, whereas $v^{1,\sigma}$ is orthogonal to the edge. The texture information on the surface will again be denoted by u. Assuming a correlation between geometry and texture we expect the angle between the texture gradient $\nabla_{\mathcal{M}} u^{\epsilon}$ and the direction $v^{1,\sigma}$ to be small, cf. Fig. 5. (Here, the indices ϵ and σ denote the smoothing parameters introduced in Section IV and Section V.)

We assume in the following that $|\kappa^{1,\sigma}| > |\kappa^{2,\sigma}|$ whenever $\kappa^{1,\sigma} \neq \kappa^{2,\sigma}$. Furthermore, we always choose the directions of $v^{i,\sigma}$ for $i = 1, 2$ such that

$$v^{i,\sigma} \cdot \nabla_{\mathcal{M}^\sigma} u^{\epsilon} \geq 0\,.$$

To set up a geometric evolution which is able to take into account also texture information, we choose two orthogonal directions $\tilde{v}^{1,\sigma}, \tilde{v}^{2,\sigma} \in \mathcal{T}_x\mathcal{M}$ – the expected directions normal and tangential to the edge – in every point $x \in \mathcal{M}$ as follows:

$$\left(\tilde{v}^{1,\sigma}, \tilde{v}^{2,\sigma}\right) := \begin{cases} \left(\frac{v}{\|v\|}, \frac{v^{\perp}}{\|v\|}\right),\ v \in \mathcal{T}_x\mathcal{M} \text{ arbitrary} \\ \qquad : \quad \nabla_{\mathcal{M}_\sigma} u^{\epsilon} = 0\,,\ \kappa_1 = \kappa_2 \\ \left(v\,, v^{\perp}\right), v = \frac{\alpha v^{1,\sigma} + (1-\alpha)\frac{\nabla_{\mathcal{M}_\sigma} u^{\epsilon}}{\|\nabla_{\mathcal{M}_\sigma} u^{\epsilon}\|}}{\|\alpha v^{1,\sigma} + (1-\alpha)\frac{\nabla_{\mathcal{M}_\sigma} u^{\epsilon}}{\|\nabla_{\mathcal{M}_\sigma} u^{\epsilon}\|}\|} \\ \qquad : \quad \text{otherwise} \end{cases},$$

where $v^{\perp}$ is a vector orthogonal to v with $\|v\| = \|v^{\perp}\|$ and $\alpha : \mathbb{R}_0^+ \to [0,1]$ is a monotone decreasing blending function depending on the ratio $|\kappa^{1,\sigma}/\kappa^{2,\sigma}|$. It returns 1 for $|\kappa^{1,\sigma}/\kappa^{2,\sigma}| \geq 1+\eta$ and 0 for $|\kappa^{1,\sigma}/\kappa^{2,\sigma}| = 1$. Hence α is responsible for a blending from the frame $(v^{1,\sigma}, v^{2,\sigma})$ to the frame $(w, w^{\perp})$ with $w = \nabla_{\mathcal{M}_\sigma} u^{\epsilon}/|\nabla_{\mathcal{M}_\sigma} u^{\epsilon}|$.

If the edge is already been classified via the shape operator $S^{\sigma}_{\mathcal{T}_x\mathcal{M}}$ we pick up directions close to those chosen in the pure geometric evolution problem. Alternatively for "softer" geometric edges - those not clearly classified via $\kappa^{1,\sigma}$ and $\kappa^{2,\sigma}$ with $\|\kappa^{1,\sigma}\| \gg \|\kappa^{2,\sigma}\|$ - we assume the texture gradient to be the canonical candidate for the direction perpendicular to a geometric edge on the surface.

The projection of the texture gradient $\nabla_{\mathcal{M}} u^{\epsilon}$ in the directions $\tilde{v}^{i,\sigma}$ will be denoted by

$$\nabla_{\mathcal{M}} u^{\epsilon,i} := \left\langle \nabla_{\mathcal{M}} u^{\epsilon}\,, \tilde{v}^{i,\sigma} \right\rangle \tilde{v}^{i,\sigma}\,.$$

As geometric diffusion problem for the surface coordinates $x \in \mathcal{M}(t)$ we now choose

$$\begin{aligned} \partial_t x - \Pi_{(T_x\mathcal{M})^{\perp}} \operatorname{div}_{\mathcal{M}}\left(a_G(S^{\sigma}, \nabla_{\mathcal{M}} u^{\epsilon})\, \nabla_{\mathcal{M}} x\right) &= 0 \\ \mathcal{M}(0) &= \mathcal{M}_0\,, \end{aligned} \tag{24}$$

where the diffusion coefficient in the basis $\tilde{v}^{1,\sigma}, \tilde{v}^{2,\sigma}$ is given by

$$a_G = \begin{pmatrix} G_G\left(\frac{\kappa^{1,\sigma}}{\lambda}, \frac{\|\nabla_{\mathcal{M}} u^{\epsilon,1}\|}{\mu}\right) & 0 \\ 0 & G_G\left(\frac{\kappa^{2,\sigma}}{\lambda}, \frac{\|\nabla_{\mathcal{M}} u^{\epsilon,2}\|}{\mu}\right) \end{pmatrix}, \tag{25}$$

and G_G is defined as

$$G_G(s,t) = \frac{1}{1+s^2+t^2}\,.$$

Hence, in the case $\nabla_{\mathcal{M}} u^{\epsilon} = 0$ we get back the diffusion coefficient of the pure geometric evolution problem (19), whereas in case $\kappa_1^{\sigma} = \kappa_2^{\sigma} = 0$ we obtain a diffusion coefficient which takes into account an anisotropy related to the texture gradient (16).

In Fig. 4 a test case for the evolution (24) is depicted. In time geometry edges develop on an initially smooth surface due to the dependency of the diffusion coefficient on the texture gradient.

Respecting geometric features in the texture evolution

Next, the formulation of a diffusion model for the texture u also takes into account information about the geometric features on the surface. We proceed in an analogous way like above. Again we define an orthonormal basis $\{w, w^{\perp}\} \subset \mathcal{T}_x\mathcal{M}$ in ev-

Fig. 7. *A surface obtained from a laser scan with an onscribed photographic texture (top left) and the same surface with moderate superimposed, isotropic noise (top right) are depicted. The latter one is considered as initial surface for the combined geometry and texture evolution. In the second row we compare results of the pure geometry evolution (left) and the combined model (right). Furthermore, two areas with characteristic differences are magnified (on the remaining left column the left eye and on the right column the mouth region). In the third row the original noisy subregions are shown, whereas in the fourth and fifth row we have depicted magnified results of the pure geometry evolution and the combined evolution, respectively. Always the same evolution timestep* $t = 0.00012$ *is considered.*

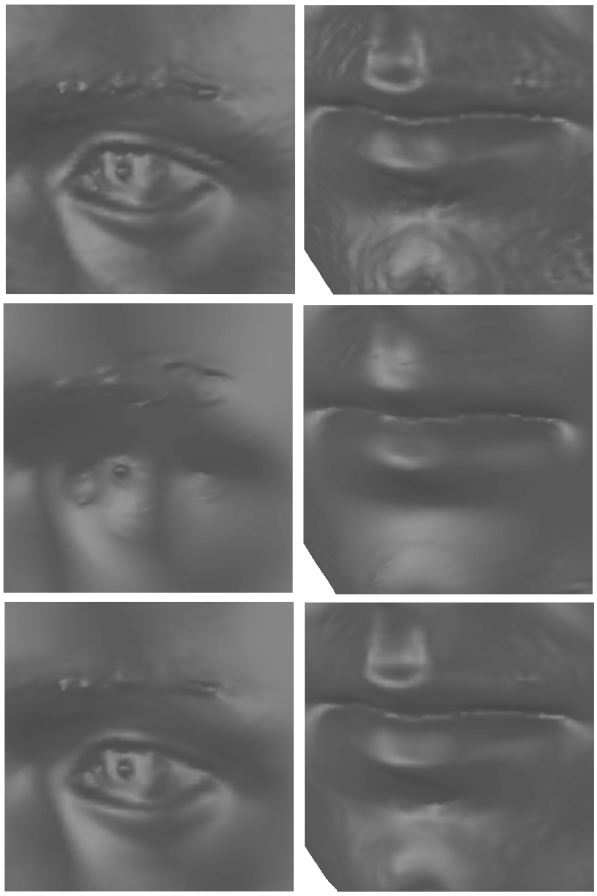

Fig. 8. *Further fairing results corresponding to the third, fourth and fifth row of Figure 7 are shown. Now they correspond to the actual 3D scanning output (cf. top left image in Figure 7) without any additional noise. On the left, we depict the subregion arround the eye of the initial surface (top) and the results of the pure geometric evolution (middle) and the coupled texture - geometry evolution respectively. On the right the corresponding results for the mouth region are shown. The time step* $t = 0.00003$ *is even smaller than the one considered in Fig. 7. All surfaces are shown without color information here, not to hide the significant changes in the geometry by texturing. Indeed, let us emphasis that the superimposed texture in Fig. 7 visually covers larger artifacts in the pure geometry evolution (cf. especially the left image in the* 2*nd row and the images in the fourth row of Fig. 7).*

ery point of $\mathcal{M}$ by

$$\left(w, w^{\perp}\right) := \begin{cases} \left(\frac{v}{\|v\|}\,,\,\frac{v^{\perp}}{\|v\|}\right), \; v \in T_p\mathcal{M} \text{ arbitrary} \\ \qquad : \quad \kappa^{1,\sigma} = \kappa^{2,\sigma}\,,\; \nabla_{\mathcal{M}} u^{\epsilon} = 0 \\ \left(v\,,v^{\perp}\right),\; v = \frac{\beta \frac{\nabla_{\mathcal{M}_\sigma} u^{\epsilon}}{\|\nabla_{\mathcal{M}_\sigma} u^{\epsilon}\|} + (1-\beta) v^{1,\sigma}}{\|\beta \frac{\nabla_{\mathcal{M}_\sigma} u^{\epsilon}}{\|\nabla_{\mathcal{M}_\sigma} u^{\epsilon}\|} + (1-\beta) v^{1,\sigma}\|} \\ \qquad : \quad \text{otherwise} \end{cases}$$

The blending function β now depends on $||\nabla_{\mathcal{M}_\sigma} u^{\epsilon}||$. It is assumed to be monotone increasing, β equals 1 for $||\nabla_{\mathcal{M}} u^{\epsilon}|| \geq \eta$, and $\beta(0) = 0$.

The projections of the two principal directions of curvature $v^{i,\sigma,\pi}$ onto the directions $w, w^{\perp} \in \mathcal{T}_x\mathcal{M}$ are denoted by

$$\begin{aligned} v^{i,\sigma\|} &:= \left\langle v^{i,\sigma}\,, w\right\rangle w \\ v^{i,\sigma\perp} &:= \left\langle v^{i,\sigma}\,, w^{\perp}\right\rangle w^{\perp}\,, \end{aligned}$$

cf. Fig. 6.

Based on the pairs $(v^{1,\sigma\|}, v^{1,\sigma\perp})$ and $(v^{2,\sigma\|}, v^{2,\sigma\perp})$ we deduce directions $v^{\|}$, $v^{\perp}$ parallel, respectively perpendicular to w whose length is weighted by the corresponding principal curvatures:

$$\begin{aligned} v^{\|} &:= \kappa^{1,\sigma} v^{1,\sigma\|} + \kappa^{2,\sigma} v^{2,\sigma\|} \\ v^{\perp} &:= \kappa^{1,\sigma} v^{1,\sigma\perp} + \kappa^{2,\sigma} v^{2,\sigma\perp}, \end{aligned}$$

Now we prescribe the diffusion problem for the texture $u : \mathcal{M} \to \mathbb{R}$ on the surface as

$$\begin{aligned} \partial_t u - \operatorname{div}_{\mathcal{M}}\big(a_T(\nabla_{\mathcal{M}} u^{\epsilon}, S^{\sigma})\, \nabla_{\mathcal{M}} u\big) &= 0 \\ u(0) &= u_0 \end{aligned} \tag{26}$$

where the diffusion coefficient in the basis $(w, w^{\perp})$ is given by

$$a_T = \begin{pmatrix} G_T\left(\frac{\|v^{\|}\|}{\lambda}, \frac{\|\nabla_{\mathcal{M}} u^{\epsilon}\|}{\mu}\right) & 0 \\ 0 & G_T\left(\frac{\|v^{\perp}\|}{\lambda}, 0\right) \end{pmatrix}.$$

with

$$G_T(s,t) = \frac{1}{1+s^2+t^2}.$$

Let us summarize the modeling of the combined anisotropic diffusion method. The shape of the diffusion coefficients a_G and a_T results in an additional sharpening of edges in the geometry in areas of high texture gradients and vice versa of edges in the texture in areas of aligned principal directions of curvature. Here by alignment we mean nearly parallel texture gradient and principal direction of curvature corresponding to the curvature with the largest absolute value.

Furthermore, in case of a locally flat surface with $\kappa^{1,\sigma} = \kappa^{2,\sigma} = 0$ we locally obtain a pure texture diffusion. On the other hand in case of a locally constant texture indicated by $\nabla_{\mathcal{M}} u^{\epsilon} = 0$ and either $\kappa^{1,\sigma}/\kappa^{2,\sigma} > 1+\eta$ or $\kappa^{1,\sigma} = \kappa^{2,\sigma}$ we locally get back to the pure anisotropic geometry diffusion.

Different from the pure geometric diffusion problem, the projection of the divergence term onto the normal space $(\mathcal{T}_x\mathcal{M})^{\perp}$ in equation (24) now suppresses a tangential shift of the surface coordinates and avoids a distortion of the associated texture information on the surface. Thus it is not only relevant for implementational purposes but already essential in the modeling.

Dependent on the application one might also be interested in other diffusion coefficients, which for example could result in an additional smoothing of the geometry in areas of low texture gradients instead of the additional sharpening of geometry edges in areas of high texture gradients. Such modifications are straightforward to incorporate based on the general approach presented here.

We have applied the combined diffusion method (24), (26) and the pure geometric diffusion method (22) to the surface of a human head. This data set was generated by a laser scanner with an additional photography unit. Fig. 7 and Fig. 8 demonstrate that the combined diffusion method is characterized by a significantly better sharpening of edges, geometric ones on the surface as well as texture edges in the texture map. To underline this we study the case with (cf. Figure 7) and without (cf. Figure 8) additional noise added to the true surface as delivered by the scanner. This is related to the fact that in this typical application we observe strong correlation of both types of features surface edges and texture edges as on most natural surfaces.

VIII. Discretization

Up to now we have considered surfaces $\mathcal{M}$ and textures u which are continuous manifolds and texture intensity functions, respectively. Concerning the implementation of the proposed multiscale method we now discretize our model. We use for both evolution problems a finite element discretization. To clarify the notation we will always denote discrete quantities with upper case letters to distinguish them from the corresponding continuous quantities in lower case letters. In the application surfaces are typically represented by triangular meshes. Hence, we suppose our meshes to be triangulations as well. Let us denote such a discrete surface $\mathcal{M}_h$. For the ease of presentation we will assume that textures are represented by piecewise linear continuous finite element functions on the same triangulation. Hence, we are interested in a family of discrete successively smoothed and sharpened surfaces and corresponding texture maps starting from some initially given noisy surface $\mathcal{M}_{h,0}$ and an initial texture U_0, respectively. We suppose all discrete surfaces to be equivalent with respect to a unique topological triangulation

$$\mathcal{T} = \{T_i \,|\, i \in I\},$$

where I is some index set. For the sake of convenience, we identify a discrete surface and its triangulation. Here the subscript h indicates the grid size, which we regard as a piecewise constant function on the current triangulation. Its value on a triangle is supposed to be the length of the longest edge. On $\mathcal{T}$ and therefore also on $\mathcal{M}_h$ we define the space of piecewise linear continuous functions

$$V^h = \{\Phi \in C^0(\mathcal{M}_h) \,|\, \Phi_{|T_i} \in \mathcal{P}_1 \,\forall i \in I\},$$

where $\mathcal{P}_1$ is the space of linear polynomials. The identity $\mathrm{Id}(\mathcal{M}_h)$ on the triangulation $\mathcal{M}_h$, which coincides with the pointwise coordinate vector X, can be regarded as a function in $(V^h)^3$. Furthermore, a discrete texture map U is also a function in V^h. Here, we consider every reference map from a single reference triangle $\hat{T} \subset \mathbb{R}^2$ onto some T_i on $\mathcal{M}_h$ as a coordinate map. Integration over $\mathcal{M}_h$ is defined in analogy to the continuous case summing over local contributions on the triangles of the mesh. The metric and the gradients of functions on $\mathcal{M}_h$ are evaluated accordingly on each triangle T.

Now we are able to formulate our discrete problem (cf. (22) for the continuous case). Discretizing first only in space we obtain a variational formulation of an evolution problem for a family $\{\mathcal{M}_h(t)\}$ of discrete surfaces with coordinate maps $X(t)$ and an evolution problem for the corresponding texture maps $U(t)$. In analogy to (21) we obtain

$$\begin{aligned} \partial_t X &= \langle V, N\rangle N, \text{ where} \\ (V,\Theta)^h_{\mathcal{M}_h} &= -(A^{\sigma}\nabla_{\mathcal{M}_h} X, \nabla_{\mathcal{M}_h}\Theta)_{\mathcal{T}\mathcal{M}_h} + (F,\Theta)_{\mathcal{M}_h} \\ (\partial_t U, \Psi)^h_{\mathcal{M}_h} &= -(B^{\epsilon}\nabla_{\mathcal{M}_h} U, \nabla_{\mathcal{M}_h}\Psi)_{\mathcal{T}\mathcal{M}_h} \end{aligned}$$

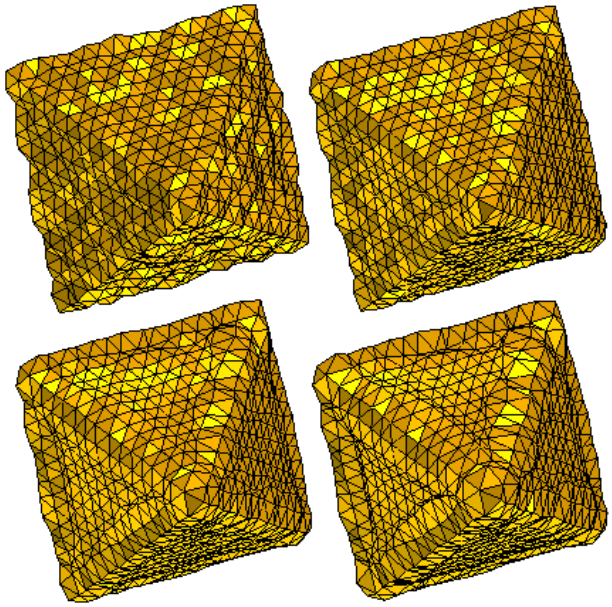

Fig. 9. *Triangular grids at different timesteps of the anisotropic evolution* (17). *The above evolution process works without projection onto the surface normals and hence is characterized by a tangential shift of the vertices, cf. the discussion Section III and Fig.* 10.

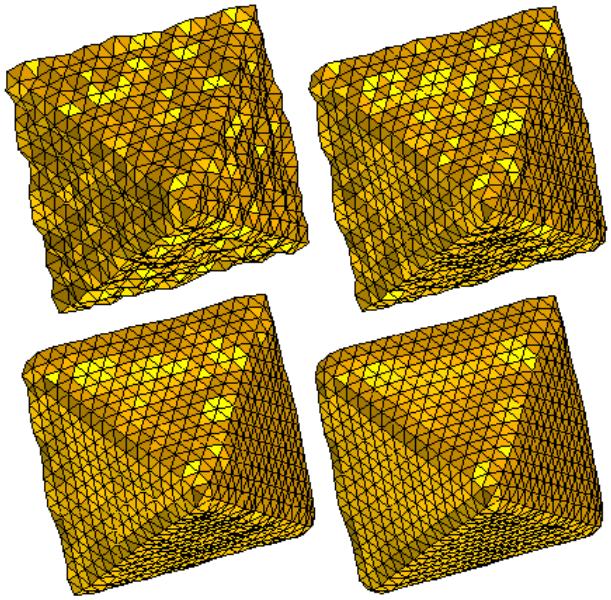

Fig. 10. *Here the evolution of the initial surface from Fig. 9 is shown using the model defined by equation (22) which suppresses tangential shifts of the surface coordinates. Thus the tangential drift of the vertices is drastically reduced in comparison to Fig. 9.*

for all test functions $\Theta \in (V^h)^3$, $\Psi \in V^h$ and initial conditions $\mathcal{M}_h(0) = \mathcal{M}_{h,0}$, $U(0) = U_0$. Here, we use the lumped mass scalar product $(\cdot,\cdot)^h_{\mathcal{M}_h}$, which is the geometric counterpart of the lumped masses for standard parabolic problems on domains in $\mathbb{R}^2$. As an immediate consequence the mass matrix is diagonal. This simplifies the resulting scheme significantly. Furthermore, F is an approximation of the volume conserving force f. We either choose $F(X) = C(X^0 - X)$ in case of the retrieving force (which has to be evaluated only at the nodes of the current triangulation due to the selected lumped mass integration formula) or the constant force $F(X) = \frac{1}{|\mathcal{M}_h|} \int_{\mathcal{M}_h} \operatorname{tr}(A^\sigma \circ S_\sigma)\, \mathrm{d}x\, N(X)$, which corresponds to the volume preserving evolution in the continuous model (compare the force in (23)). Here, S_σ denotes a discrete shape operator. As a discrete interpolated normal $N(X)$ on the nodes of the triangulation we consider a weighted sum of the adjacent triangle normals. As weights we choose the area of the corresponding triangle. Our discrete anisotropic diffusion tensors A^σ and B^ϵ, to be defined later, are supposed to be endomorphisms on the discrete tangent bundle $\mathcal{T}\mathcal{M}_h(t)$ approximating the continuous tensors a^σ and b^ϵ, respectively. We end up with a system of ordinary differential equations for the three coordinates of all triangulation nodes and the nodal values of the texture map.

Next, we have to discretize in time, which includes the choice of some timestepping scheme and the decision which terms to be handled implicitly and which explicitly. Here we proceed in analogy to the approach presented by Dziuk [12] for the discretization of mean curvature motion. We expect X^n and U^n to be approximations of $X(n\tau)$ and $U(n\tau)$, respectively, where τ is the selected timestep. Now, the time derivative is discretized applying a backward Euler scheme

$$\partial_t X((n+1)\tau) \approx \frac{X^{n+1} - X^n}{\tau}.$$

Finally, we obtain the following fully discrete problem:

Find a sequence $\{X^n_h\}_{n=0,\dots} \subset (V^h)^3$ of discrete coordinate maps which defines a family of triangular surfaces $\{\mathcal{M}^n_h\}_{n=0,\dots}$ and a sequence of discrete texture maps $\{U^n_h\}_{n=0,\dots} \subset V^h$ such that

$$X^{n+1} = X^n + \tau \left\langle V^{n+1}, N^n \right\rangle N^n, \text{ with}$$

$$\left(V^{n+1}, \Theta\right)^h_{\mathcal{M}^n_h} + \left(A^\sigma_n \nabla_{\mathcal{M}^n_h}(X^n + \tau V^{n+1}), \nabla_{\mathcal{M}^n_h}\Theta\right)_{\mathcal{T}\mathcal{M}^n_h} = \left(F^n, \Theta\right)_{\mathcal{M}^n_h} \text{ and}$$

$$\left(\frac{U^{n+1} - U^n}{\tau}, \Psi\right)^h_{\mathcal{M}^n_h} + (B^\epsilon_n \nabla_{\mathcal{M}^n_h} U^{n+1}, \nabla_{\mathcal{M}^n_h}\Psi)_{\mathcal{T}\mathcal{M}^n_h} = 0$$

for all discrete test functions $\Theta \in (V^h)^3$ and $\Psi \in V^h$.

Fig. 9 and 10 show the evolving finite element meshes under the discrete flow excluding and including the projection of the velocity field V^{n+1} in direction of the normal field N^n, respectively. In what follows we explain in detail the notation used above and discuss at which timestep to evaluate functions, metric and diffusion tensor. As the governing metric we always consider the one at the old timestep, here indicated by the superscripts in $\mathcal{M}^n_h$ and $\mathcal{T}\mathcal{M}^n_h$. Thus, also the gradients $\nabla_{\mathcal{M}^n_h}$ are considered with respect to the metric on $\mathcal{T}\mathcal{M}^n_h$. Furthermore, the diffusion tensors A^σ and B^ϵ are evaluated explicitly at time $t_n = n\tau$, which we indicate by a lower index n. Concerning the right hand side, we also evaluate F at the old time t_n and define $F^n = F(t_n)$. Finally, in each step of the discrete evolution we have to solve four systems of linear equations. Up to the right

hand side, three times the same system for the three coordinate components and one system for the discrete evolution of the texture have to be solved in each timestep. Let us now focus on the geometric evolution problem. In terms of nodal vectors, which we indicate by a bar on top of the corresponding discrete function we can rewrite the scheme and get in matrix formulation

$$\begin{aligned} \bar{X}^{n+1} &= \bar{X}^n + \tau \langle \bar{V}^{n+1}, \bar{N}^n \rangle \bar{N}^n \\ (M^n + \tau L^n(A_n^\sigma))\, \bar{V}^{n+1} &= M^n \bar{F}^n - L^n(A_n^\sigma)\bar{X}^n \\ (M^n + \tau L^n(B_n^\epsilon))\, \bar{U}^{n+1} &= -L^n(A_n^\sigma)\bar{U}^n \end{aligned} \tag{27}$$

for the new velocities $\bar{V}^{n+1}$, the new vertex positions $\bar{X}^{n+1}$ and the new texture map values $\bar{U}^{n+1}$ at time $t_{n+1} = (n+1)\tau$. Here, we assume the lumped mass matrix

$$M^n = \left((\Phi_i, \Phi_j)^h_{\mathcal{M}_h^n} \right)_{ij}$$

and the nonlinear stiffness matrix

$$L^n(A_n^\sigma) = \left((A_n^\sigma \nabla_{\mathcal{M}_h^n} \Phi_i, \nabla_{\mathcal{M}_h^n} \Phi_j)_{\mathcal{T}\mathcal{M}_h^n} \right)_{ij}$$

to be applied simultaneously to each of the three coordinate components. The set $\{\Phi_i, i \in I\}$ is the canonical basis of V^h. If in addition a nonvanishing right-hand side is considered, we have to evaluate the vector $\bar{F}^n$ representing the right-hand side on each node X, i. e. $(\bar{F}^n)_i = F^n(X_i^n)$. The diffusion tensor A_n^σ is supposed to be piecewise constant on the triangles of our mesh. As in the continuous model the evaluation of the diffusion tensor has to be based on a regularized, prefiltered surface. Here we consider a single timestep of the discrete mean curvature evolution as an appropriate geometric regularization and a timestep of linear diffusion as a regularization of the texture information, i. e. we compute

$$\begin{aligned} \bar{X}_\sigma^n &= \left(M^n + \frac{\sigma^2}{2} L^n(\mathrm{Id}) \right)^{-1} \bar{X}^n \\ \bar{U}_\sigma^n &= \left(M^n + \frac{\sigma^2}{2} L^n(\mathrm{Id}) \right)^{-1} \bar{U}^n \end{aligned} \tag{28}$$

where $L^n(\mathrm{Id})$ is the above stiffness matrix for the isotropic diffusion tensor Id. Then the corresponding coordinate map X_σ^n defines a discrete surface $\mathcal{M}_{h,\sigma}^n$. Thus, we have filtered the probably noisy initial coordinates and texture values with a "geometric" and discrete Gaussian filter of width σ before we identify edges to be enhanced by our actual discrete evolution. Hence, high frequency noise is suppressed and we obtain well-posed discrete problems whose asymptotic behaviour is independent of the grid size. Let us emphasize that we apply this regularization filters only to evaluate the diffusion tensors and not as an evolution step of the surface or texture itself. The required solver for this smoothing problem is already available by a slight modification of our original scheme for a single timestep.

In the continuous model a suitable construction of a diffusion tensor, which incorporates edge sharpening and tangential smoothing along edges, involves the principal curvatures and principal directions of curvature deduced from the shape operator. Now in the discrete case, we are interested in some discrete

Fig. 11. *The initial surface (top left) and three timesteps from the evolution (22) of a venus head consisting of* 268714 *triangles are shown. The evolution times are* 0.00005, 0.0001, *and* 0.0002 *and the parameters are* $\lambda = 10$, $\sigma = 0.02$.

counterpart. At first, triangulated surfaces have no canonical curvature tensor. For every triangle T the curvature evaluation is based on local L^2-projections of the triangulated and regularized surface $\mathcal{M}_{h,\sigma}^n$ onto graphs of quadratic polynomials over the tangent space. In our case the embedded tangent space coincides with the plane containing T. For these polynomials the corresponding shape operator S_σ^n can be computed explicitly. For details we refer to Section IX. Finally, we evaluate the required diffusion tensor A_n^σ on every triangle T by (see (19) and (20))

$$A_n^\sigma|_T = a^\sigma_{\mathcal{T}_x\mathcal{M}}(S_n^\sigma)\,,$$

where we take up our original definition (cf. Section V) for the continuous problem and apply it now to the numerical approximation S_n^σ of the continuous operator $S^\sigma_{\mathcal{T}_x\mathcal{M}_\sigma}$.

Figure 11 shows an initial surface and results from the semi-implicit algorithm for a venus head data set. Figure 12 gives a comparison of the evolution results at time $t = 0.00005$ for different prefilter width values σ. Finally, in Fig. 13 we compare the dependence of the solution on the parameter λ. For smaller values of λ more and more feature edges are enhanced. Here we consider the data set from Fig. 1. The initial diameter of the object is always set to 1.

IX. Curvature on a discrete surface

Let T be an element of a triangulation $\mathcal{M}_h$ with vertices P^1, P^2, P^3 and barycenter $C_T = \frac{1}{3}(P^1 + P^2 + P^3)$. The normal

Fig. 12. *The discrete solutions of (22) at time $t = 0.00005$ are calculated for different values of the prefilter width ($\sigma = 0.005$ (left) and $\sigma = 0.08$ (right)).*

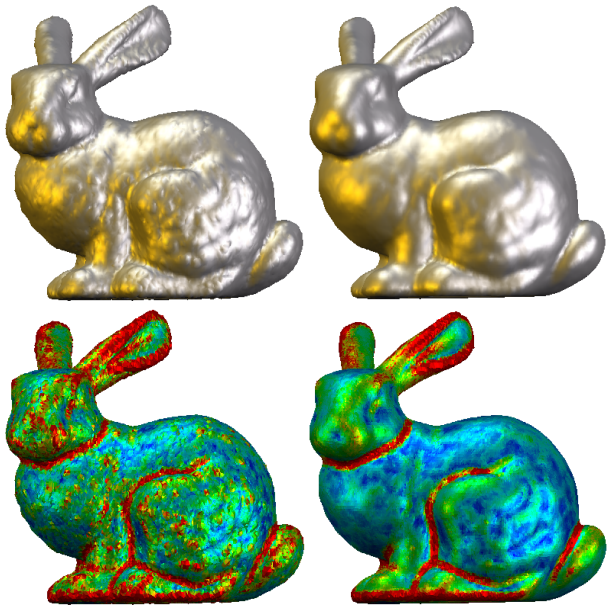

Fig. 13. *For $\lambda = 10$ (left) and $\lambda = 30$ (right) the discrete solutions of (22) are shown at time $t = 0.0001$. In the bottom row the dominant principal curvature corresponding to the surfaces above are depicted in color.*

Fig. 14. *The dominant principal curvature is color coded for the evolution sequence shown in Figure 11.*

$$\sum_j \left(\int_{\hat{\omega}_T} \varphi_i \varphi_j dxdy \right) \Xi_j = \int_{\hat{\omega}_T} \varphi \varphi_i dxdy,\ i = 1, \ldots, 6\,.$$

Finally, the discrete principal curvatures κ_1, κ_2 and the principal directions of curvature of $\mathcal{M}_h$ on T are defined as the corresponding quantities for the smooth surface $(x, y, p(x, y))$ in the origin.

of T is denoted by N. First we assume a normalized setting with $C_T = 0$ and $N = (0, 0, 1)$, i.e. $P^1, P^2, P^3 \in \{z = 0\}$, where points in $\mathbb{R}^3$ are denoted by (x, y, z). This can be obtained by rotation with some matrix $Q \in SO(3)$ and translation.

We will now assume that $\omega_T = \{T' \in \mathcal{M}_h \,|\, T' \cap T \neq \emptyset\}$ is given as a graph over the plane $\{z = 0\}$. This is expected to hold true if a smooth manifold $\mathcal{M}$ is discretized with a sufficiently small gridsize h. If, however, ω_T is not a graph over the plane $\{z = 0\}$ the following method does not break down but it may lead to meanigless discrete curvatures. The image of the projection of ω_T on $\{z = 0\}$ is denoted by $\hat{\omega}_T$. Then the graph ω_T is represented by a piecewise linear function $\varphi : \hat{\omega}_T \to \mathbb{R}$. Now we compute the $L^2(\hat{\omega}_T)$-projection of φ onto the space of quadratic polynomials $\mathcal{P}_2$. To this end, let $p(x, y) = \alpha x^2 + \beta xy + \gamma y^2 + \delta x + \zeta y + \eta$ be this $\mathcal{P}_2$-function, characterized by $\Xi = (\alpha, \beta, \gamma, \delta, \zeta, \eta) \in \mathbb{R}^6$ and let $\varphi_1 = x^2, \varphi_2 = xy, \varphi_3 = y^2, \varphi_4 = x, \varphi_5 = y, \varphi_6 = 1$ be the canonical basis of $\mathcal{P}_2$. Then Ξ is given by the linear equation

X. Comparison and conclusions

We have presented a novel coupled multiscale method for surface fairing and texture denoising. It is able to successively smooth noisy initial surfaces with onscribed texture information while simultaneously enhancing edges and corners of the surface and edge type features of the texture maps. The evolution time plays the role of the scale parameter.

The method is based on an anisotropic curvature evolution problem. The corresponding nonlinear partial differential equations have been discretized by finite elements in space and a semi implicit backward Euler scheme in time. A projection approach has been considered to cope with the tangential shifts due to the nonvanishing divergence of the anisotropy in the presented model. The method allows the efficient and flexible processing of arbitrary triangulated surfaces and accompanying texture maps, as they are common in geometric modeling and computer graphics applications. The user controls the surface evolution mainly by four parameters which have an intuitive meaning.

Two regularization parameters σ, ϵ have to be chosen to filter out high frequency noise in the geometry and texture before the diffusion coefficients are evaluated. Here a suitable choice in the application is $\sigma = Ch$ with $C \in [1, 4]$ and $\epsilon = Kh$ with $K \in [0, 1]$. Furthermore, λ and μ can be regarded as user given threshold values for the edge detection on the surface and on the texture intensity map, respectively.

Interesting future research directions are

- the combination of the presented multiscale method with multiresolutional techniques, which should appropriately reflect the continuous coarsening in the evolution,
- further investigations on surface modeling concerning suitable choices of the diffusion tensor and the forcing on the right hand side of the parabolic system, and
- investigations concerning a natural energy quantity, such that evolution problems of the kind considered here are gradient flows of this energy, as it is known for cristalline anisotropic curvature flow [32].

Additional material and high resolution pictures of the figures contained in this paper are available at *http://numerik.math.uni-duisburg.de*.

Acknowledgement

The authors thank Martin Roth from the ETH Zurich for providing the facial dataset containing texture information used in this paper.

REFERENCES

[1] M. Desbrun, M. Meyer, P. Schroeder, and A. Barr, "Implicit fairing of irregular meshes using diffusion and curvature flow," in *Computer Graphics (SIGGRAPH '99 Proceedings)*, 1999, pp. 317–324.

[2] L. Kobbelt, "Discrete fairing," in *Proceedings of the 7th IMA Conference on the Mathematics of Surfaces*, 1997, pp. 101–131.

[3] L. Kobbelt, S. Campagna, J. Vorsatz, and H.-P. Seidel, "Interactive multiresolution modeling on arbitrary meshes," in *Computer Graphics (SIGGRAPH '98 Proceedings)*, 1998, pp. 105–114.

[4] G. Taubin, "A signal processing approach to fair surface design," in *Computer Graphics (SIGGRAPH '95 Proceedings)*, 1995, pp. 351–358.

[5] B. Curless and M. Levoy, "A volumetric method for building complex models from range images," in *Computer Graphics (SIGGRAPH '96 Proceedings)*, 1996, pp. 303–312.

[6] W.E. Lorensen and H.E. Cline, "Marching cubes: A high resolution 3d surface construction algorithm," *Computer Graphics*, vol. 21, no. 4, pp. 163–169, 1987.

[7] M. P. do Carmo, *Riemannian Geometry*, Birkhäuser, Boston–Basel–Berlin, 1993.

[8] I. Chavel, *Eigenvalues in Riemannian Geometry*, Academic Press, 1984.

[9] V. Thomée, *Galerkin - Finite Element Methods for Parabolic Problems*, Springer, 1984.

[10] I. Guskov, W. Sweldens, and P. Schroeder, "Multiresolution signal processing for meshes," in *Computer Graphics (SIGGRAPH '99 Proceedings)*, 1999.

[11] U. Dierkes, S. Hildebrandt, A. Küster, and O. Wohlrab, *Minimal Surfaces*, Grundlehren der Mathematischen Wissenschaften. 295. Berlin: Springer-Verlag, 1992.

[12] G. Dziuk, "An algorithm for evolutionary surfaces," *Numer. Math.*, vol. 58, pp. 603–611, 1991.

[13] P. Perona and J. Malik, "Scale space and edge detection using anisotropic diffusion," in *IEEE Computer Society Workshop on Computer Vision*, 1987.

[14] B. Kawohl and N. Kutev, "Maximum and comparison principle for one-dimensional anisotropic diffusion.," *Math. Ann.*, vol. 311 (1), pp. 107–123, 1998.

[15] L. Alvarez, F. Guichard, P. L. Lions, and J. M. Morel, "Axioms and fundamental equations of image processing," *Arch. Ration. Mech. Anal.*, vol. 123, pp. 199–257, 1993.

[16] F. Catté, P. L. Lions, J. M. Morel, and T. Coll, "Image selective smoothing and edge detection by nonlinear diffusion," *SIAM J. Numer. Anal.*, vol. 29, pp. 182–193, 1992.

[17] J. Weickert, "Foundations and applications of nonlinear anisotropic diffusion filtering," *Z. Angew. Math. Mech.*, vol. 76, pp. 283–286, 1996.

[18] T. Preußer and M. Rumpf, "Anisotropic nonlinear diffusion in flow visualization," in *Proceedings Visualization 1999*, 1999.

[19] R. Kimmel, "Intrinsic scale space for images on surfaces: The geodesic curvature flow," *Graphical Models and Image Processing*, vol. 59(5), pp. 365–372, 1997.

[20] G. Sapiro, *Geometric Partial Differential Equations and Image Processing*, Cambridge University Press, 2001.

[21] J. Weickert, *Anisotropic diffusion in image processing*, Teubner, 1998.

[22] J. Kačur and K Mikula, "Solution of nonlinear diffusion appearing in image smoothing and edge detection," *Appl. Numer. Math.*, vol. 17, pp. 47–59, 1995.

[23] E. Bänsch and K. Mikula, "A coarsening finite element strategy in image selective smoothing," *Computing and Visualization in Science*, vol. 1, pp. 53–63, 1997.

[24] T. Preußer and M. Rumpf, "An adaptive finite element method for large scale image processing," in *Scale-Space Theories in Computer Vision*, 1999, pp. 232–234.

[25] T. Preußer and M. Rumpf, "A level set method for anisotropic geometric diffusion in 3D image processing," *To appear in SIAM J. Appl.*, 2002.

[26] J. Weickert, "Theoretical foundations of anisotropic diffusion in image processing," *Computing*, vol. Suppl. 11, pp. 221–236, 1996.

[27] U. Diewald, U. Clarenz, and M. Rumpf, "Nonlinear anisotropic diffusion in surface processing," in *Proceedings of IEEE Visualization 2000*, 2000, pp. 397–405.

[28] U. Clarenz, "Enclosure theorems for extremals of elliptic parametric functionals," *Calc. Var., online publication DOI 10.1007/s005260100128*, 2001.

[29] G. Huisken, "The volume preserving mean curvature flow.," *J. Reine Angew. Math.*, vol. 382, pp. 35–48, 1987.

[30] J. Weickert, "Coherence-enhancing diffusion of colour images," *Image and Vision Computing*, vol. 17, pp. 201–212, 1999.

[31] J. D. Foley, A. van Dam, S. K. Feiner, and J. F. Hughes, *Computer Graphics: Principles and Practice*, Addison-Wesley, 1990.

[32] G. Belletini and M. Paolini, "Anisotropic motion by mean curvature in the context of finsler geometry," *Hokkaido Math. J.*, vol. 25, pp. 537–566, 1996.